Published in final edited form as:
Colloids Surf B Biointerfaces. 2008 July 15; 64(2): 236–247.

MC3T3-E1 Cell Adhesion to Hydroxyapatite with Adsorbed Bone Sialoprotein, Bone Osteopontin, and Bovine Serum Albumin

Matthew T. Bernards[a], **Chunlin Qin**[c,*], and **Shaoyi Jiang**[a,b,*]

a *Department of Chemical Engineering, University of Washington, Seattle, WA 98195*

b *Department of Bioengineering, University of Washington, Seattle, WA 98195*

c *Department of Biomedical Sciences, Baylor College of Dentistry, Texas A&M University System Health Science Center, Dallas, TX 75246*

Abstract

Native bone tissue is composed of a complex matrix of collagen, non-collagenous proteins, and hydroxyapatite (HAP). Bone sialoprotein (BSP) and bone osteopontin (OPN) are members of the non-collagenous protein family termed the SIBLING (small integrin-binding ligand, N-linked glycoproteins) proteins, which are primarily found in mineralized tissues. Previously, OPN was shown to exhibit a preferential orientation for MC3T3-E1 cell adhesion when it was specifically bound to collagen, while the MC3T3-E1 cell adhesion was shown to be dependant on the conformational flexibility of BSP specifically bound to collagen. Additionally, OPN was shown to play a greater role than BSP for cell binding to collagen. In this work, the orientations and conformations of BSP and OPN specifically bound to HAP are probed under similar conditions. Radiolabeled adsorption isotherms were obtained for BSP and OPN on HAP formed from a simulated body fluid, and the results show that HAP has the capacity to bind significantly more BSP than OPN. An *in vitro* MC3T3-E1 cell adhesion assay was then performed to compare the cell binding ability of adsorbed BSP and OPN specifically bound to HAP. It was found that there is a preference for cell binding to HAP with adsorbed BSP as compared to OPN, but not to a statistically significant level. However, the maximum cell binding was observed on HAP substrates with adsorbed heat denatured bovine serum albumin (BSA). The influence of BSA on cell binding was shown to be concentration dependant and it is believed that the adsorbed BSA modulates the proliferation state of the bound cells.

Keywords

Bone Sialoprotein; Bone Osteopontin; Albumin; Hydroxyapatite; Orientation; Conformation

Introduction

Calcium phosphate or hydroxyapatite (HAP) based biomaterials are very prevalent in bone and dental tissue engineering due to their outstanding properties including biocompatibility, bioactivity, osteoconductivity, and similarity in composition to the mineral phases of bone and dental tissue.[1] A number of investigators are currently examining the influence of various

* Corresponding Authors: Shaoyi Jiang - sjiang@u.washington.edu; Chunlin Qin - cqin@bcd.tamhsc.edu.

calcium phosphates on the adhesion, proliferation, and differentiation of bone-related cells.[2–6] These studies are primarily focused on the influence that characteristics of the calcium phosphates, such as the surface coverage, structure, and the exact composition, have on the cells and their function. In one of these studies, Chou *et al* examined four different forms of HAP and determined that while the HAP samples induced osteoblast differentiation, there were more cells adherent on the tissue culture polystyrene controls at all of the time points examined.[2] Additionally, Ogata and co-workers found that after 12 hours of adhesion time, there were only ~50 cells/mm^2 bound to each of the types of HAP they tested. Both of these studies indicate that while HAP coatings are not toxic to cells, they are also not ideal substrates for cellular adhesion.

While calcium phosphate coatings appear to be non-ideal for cell adhesion, it may be possible to increase the adhesiveness through the binding of proteins or synthetic peptides to the surface of the mineral. Several studies have examined the adsorption characteristics of proteins or peptides to HAP or other calcium phosphate surfaces, primarily with a focus on understanding the mineralization induction or inhibition abilities of that particular protein.[7–9] Recently, Krout *et al* examined the influence that osteocalcin (OC) has on both the mineral structure and cell binding properties when it is included as a component of the mineralization solution. It was found that while there were no changes to the crystal properties, there was improved cellular adhesion to the samples through the incorporation of OC within the sample.[10] Additionally, Webster *et al* examined the influence that five different proteins and fetal bovine serum had on the adhesion of cells to both conventional and nanoscale ceramics (including HAP) and it was found that the presence of adsorbed proteins, especially vitronectin, did promote osteoblast adhesion to the ceramics.[11] While a number of proteins including OC, bone sialoprotein (BSP), osteopontin (OPN), osteonectin (ON), and bone morphogenic protein (BMP) have been found within bone tissue, only a limited number of these, in particular OPN and BSP, have been localized within the collagenous matrix ahead of the mineralization front in developing bone (i.e., in osteoid adjacent to the mineralization front).[9,12–14] This indicates that these two proteins may play a role in the osteoblast adhesion to this interfacial matrix of developing bone, which consists of primarily type 1 collagen and HAP.[1,12–15] In addition, both of these proteins have been found to be enriched at bone-implant interfaces and they are hypothesized to play an important role in cellular adhesion and osseointegration at this interface as well.[16]

OPN and BSP are both members of the SIBLING (small integrin-binding ligand, N-linked glycoproteins) family, one category of non-collagenous proteins found in many mineralized tissues. The SIBLING family members share a number of properties, including that they are secreted, phosphorylated, and sulfated sialoproteins, that are acidic in nature.[17] Depending on the species, OPN is composed of 260-317 amino acids, with a molecular weight of 45–75 kDa[18,19] and BSP is composed of 281-327 amino acids, with a molecular weight of 60–80 kDa.[20] Both proteins were originally isolated from bone matrix. Since its initial identification, OPN has been found within other tissues throughout the body, while BSP has been found to have a limited distribution outside of mineralized tissue and the immediate surroundings. The functions of these two proteins within the body have been reviewed extensively in the literature.[18–23] OPN and BSP are both known to contain an arginine-glycine-aspartic acid (RGD) motif that mediates cell binding through direct interactions with a number of transmembrane integrin pairs.[24] Additionally, both proteins have been shown to have an affinity for both calcium and collagen, which is not unexpected based on their localization in developing and mature bone, and bone-implant interfacial zones.[25,26] OPN has one poly-aspartic acid sequence and BSP has two poly-glutamic acid sequences and these sequences are believed to be responsible for the binding of these proteins to HAP.[19,20]

It is well understood that within seconds of implantation, biomaterials are coated with an adsorbed layer of proteins and it is this layer of proteins that modulates the cellular response

to the implanted material at early interaction times.[27,28] Recent efforts in biomaterials design have focused on understanding and controlling the composition, orientation, and conformation of this adsorbed layer of proteins in order to improve the wound healing process and subsequent integration of the implant material into the body.[16,29] However, controlling the orientation and conformation of adsorbed proteins is challenging. Some success has been shown for controlling protein orientation with charged self-assembled monolayers (SAMs).[30,31] The ability to control protein orientation with charged SAMs is mediated by the conformational stability and size of the adsorbed protein.[32,33] Other efforts have focused on utilizing specific protein-protein interactions to impart a natural biological orientation or conformation to one of the proteins.[34–36] Our previous efforts examined the MC3T3-E1 osteoblast-like cell binding onto both OPN and BSP covered surfaces when the proteins were randomly adsorbed to tissue culture polystyrene (TCPS) or specifically bound to collagen I.[34,36] In these studies it was found that when identical amounts of OPN was adsorbed to the two surfaces there were statistically significant differences in the cell binding to the two surfaces, indicating that OPN is given a preferential orientation or conformation for MC3T3-E1 binding when it is specifically bound to collagen I. At the same time, when equal amounts of BSP was adsorbed to the two surfaces it was found that there were no differences in the level of cell binding and this was attributed to the conformational flexibility of this protein in the area surrounding its RGD cell binding moiety. When the cellular binding characteristics of the two proteins were compared to each other, it was determined that OPN plays a greater role than BSP for MC3T3-E1 binding to collagen.

The foci of this work are (a) to determine and compare the cellular binding to HAP both in the presence or absence of adsorbed OPN or BSP over a range of HAP growth periods, and (b) to indirectly probe the orientation and conformation imparted to both OPN and BSP through their specific binding interactions with HAP by measuring the availability of the cell binding RGD moiety for binding interactions. These studies will provide valuable information regarding the roles that both of these proteins play in cellular adhesion during bone formation, especially when taken in conjunction with our previous studies involving collagen. It was hypothesized that OPN would have a more favorable orientation or conformation for cellular binding than BSP, in a manner similar to that seen between these two proteins when specifically bound to collagen.[34] In order to directly compare the influence that orientation or conformation has on the cellular binding properties of adsorbed proteins, it is essential to ensure that there are identical amounts of adsorbed proteins. This was achieved in this work via radiolabeling assays. The cellular binding properties of these two proteins were compared when they were adsorbed on HAP substrates that were formed for 1, 3, or 7 days from a simulated body fluid (SBF) [37] with an MTT cell binding assay. In these studies it was determined that BSP has a slightly higher levels of MC3T3-E1 cell binding as compared to OPN, but not to a statistically significant level. This cell binding appears to be mediated by the surface roughness of the underlying HAP. Furthermore, it was found that the maximum cellular binding was achieved on all of the HAP substrates when they were coated with adsorbed heat denatured bovine serum albumin (BSA) rather than OPN or BSP. It is hypothesized that BSA affects the proliferation state of the MC3T3-E1 cells, leading to higher levels of cell binding in this study.

Experimental Procedures

Materials

11-Mercaptoundecanoic acid [$HS(CH_2)_{10}COOH$] was purchased from Sigma (St. Louis, MO) and used as received. Glass cover slips were purchased from Fisher Scientific (Pittsburg, PA) and they were coated with a 2 nm chromium adhesion layer followed by a 20 nm gold layer using electron-beam evaporation. Tris·HCl buffer was prepared by dissolving 25 mM Tris·HCl (Sigma) and 125 mM NaCl (Sigma) in 18.2 M H_2O and adjusting the pH to 7.4 with NaOH

(Sigma). The buffer was filter sterilized with 0.22 μm vacuum filters before use. BSA with a purity of ≥96% was purchased from Sigma. Heat denatured BSA was prepared by dissolving BSA in Tris·HCl buffer and heating it at 60° C for 30 minutes. All cell culture supplies including medium, serum, and trypsin-EDTA (0.05%/0.53 mM) were purchased from Gibco (Gaithersburg, MD). The osteoblast cell line MC3T3-E1 was a gift from Dr. P. Stayton (University of Washington). All other chemicals were purchased from Sigma and used as received.

Self-Assembled Monolayer Preparation

Carboxylic acid (-COOH) terminated SAMs were prepared by the adsorption of 11-mercaptoundecanoic acid on gold-coated substrates following previously reported procedures.[38] Briefly, all gold-coated substrates were rinsed with ethanol, dried with filtered air, irradiated under ultraviolet/ozone for 30 minutes, rinsed with 18.2 M water, rinsed with ethanol, and dried with filtered air. SAMs were formed by soaking the cleaned substrates overnight in 0.5 mM alkanethiol solutions in ethanol containing 2% trifluoroacetic acid (v/v) at room temperature. Finally, the -COOH terminated SAM coated chips were washed with ethanol, a 1:10 (v/v) ethanolic solution containing ammonium hydroxide, ethanol, and 18.2 MΩ water, and dried with filtered air just prior to use.

Hydroxyapatite Formation from Simulated Body Fluid

HAP was formed on -COOH terminated SAM surfaces using Oyane *et al*'s modified SBF.[37] Briefly, the reagents listed in Table 1 were dissolved in the order they are listed in 18.2 MΩ water to form 500 mL of SBF. The SBF was then placed into a Pyrex crystallization dish and gold-coated cover slips with -COOH terminated SAMs were submerged in the SBF. 10–20 cover slips were placed in each batch of SBF (500 mL). HAP was grown for 1, 3, 7, or 14 days in a humidified atmosphere at 37° C and 5% CO_2 using separate crystallization dishes for each growth period. The SBF was replaced with fresh SBF every 2–3 days over the course of the HAP growth cycle. At the conclusion of the growth period, the SBF was removed and the HAP coated substrates were rinsed 3 times with 100 mL of deionized water, 3 times with 100 mL of 18.2 MΩ water, and dried in air prior to protein adsorption or HAP characterization.

Hydroxyapatite Characterization

The HAP was characterized with an FEI Sirion scanning electron microscope (SEM) equipped with an energy dispersed spectrometer (EDAX) system. Samples from four separate batches of SBF were characterized for each of the HAP growth periods of 1, 3, and 7 days. Imaging and elemental analyses were completed for three discrete spots on each of the samples.

Isolation of OPN and BSP from Rat Long Bone

The non-collagenous extracellular matrix (ECM) proteins were extracted from the tibiae of ~10 week old rats by standard procedures as described previously.[39,40] Briefly, the tibiae were extracted with 0.5 M EDTA in 4 M guanidium-HCl containing protease inhibitors (GdmCl; Acros Organics, Fairlawn, NJ). Next, the extracts were subjected to gel chromatography on Sephacryl S-200 in 4 M GdmCl. Using this procedure, the high molecular weight protein fraction (designated as ES1) was separated from smaller sized proteins like OC. ES1 was next chromatographed on DEAE-Sephacel, eluted with a linear gradient formed from 750 mL each of the starting buffer (50 mM Tris·HCl, 6 M urea, pH 7.2) and 50 mM Tris·HCl, 6 M urea containing 0.7 M NaCl (pH 7.2). The DEAE-Sephacel chromatography separated the ES1 bone extracts into seven major fractions.[40] The DEAE-Sephacel fractions rich in OPN and BSP were passed separately over a Bio-Gel A50m column (BIO-RAD, Hercules, CA) to further purify the OPN and BSP. For Bio-Gel A50m chromatography, a buffer consisting of 6 M urea and 50 mM Tris·HCl at pH 7.2 was used. Isolated OPN and BSP were analyzed by

polyacrylamide gel electrophoresis (SDS-PAGE) with Stains-All staining to ensure their purity. The identities of OPN and BSP were further confirmed by Western immunoblots using antibodies that were specifically reactive to OPN or BSP.

Protein Adsorption Isotherms

OPN and BSP were radiolabeled with ^{125}I using the iodine monochloride (ICI) method.[41] ^{125}I radiolabeled OPN or BSP were added to 0.5 mg/mL unlabeled OPN or BSP to obtain solutions with specific activities of 78.3 and 281.77 counts per minute (cpm) per ng protein, respectively. OPN and BSP adsorption isotherms were determined for HAP grown for a period of two weeks as discussed above. After the final drying step, HAP samples were incubated with solutions of either OPN or BSP overnight at 4° C in a humidified atmosphere. Four solution concentrations of OPN were tested and six solutions concentrations of BSP were tested. Following the protein adsorption step, all of the surfaces were rinsed three times with Tris·HCl buffer to remove loosely adhered proteins. The cpm radioactivity of all of the samples was measured with a TM Analytic 1185R Gamma Trac Gamma Counting System (Elk Grove, IL). The amount of protein bound to each of the surfaces was calculated by relating the cpm of each sample to its specific activity exposure amount and surface area.

Cell Culture

MC3T3-E1 cells were maintained in continuous growth on TCPS flasks in alpha Minimum Essential Medium (α-MEM), supplemented with 10% fetal bovine serum and 2% penicillin-streptomycin solution in a humidified atmosphere at 37° C and 5% CO_2. To passage, cells were rinsed twice with 10 mL of Tris·HCl buffer followed by incubation in 2 mL of trypsin/EDTA. After the cells detached from the TCPS flask, they were resuspended in supplemented medium and replated onto new TCPS flasks. Cells were passaged once a week and passages 4–7 were used for experiments.

Cell Adhesion with BSA Blocking

The cell adhesion assay is similar to that described previously with minor modifications.[34, 36,42] The protein adsorption procedure was similar to that described above for the radiolabeled protein adsorption isotherm. However, only one specific protein concentration was used for each protein that was examined and only native (non-radiolabeled) protein was used. HAP and SAM coated substrates were prepared and then exposed to either 50 μg/mL of OPN or 35 μg/mL of BSP overnight at 4° C in a humidified atmosphere. Control samples were prepared for all of the substrates by incubating them with 1 mg/mL of heat denatured BSA. Following the overnight protein adsorption, the samples were transferred to a 24-well culture plate where they were rinsed three times with 1 mL of Tris·HCl buffer and then blocked with 1 mL of heat denatured BSA for 30 minutes. In the meantime, freshly confluent MC3T3-E1 cells were detached with 2 mL of trypsin/EDTA and resuspended in 5 mL of 5 mg/mL soybean trypsin inhibitor in PBS. The cells were centrifuged at 1000 rpm for 7.5 minutes, after which the supernatant was removed and the cells were washed twice with 5 mL of 5 mg/mL BSA in non-supplemented (serum free) α-MEM. Following this step, the cells were resuspended in serum free α-MEM and diluted to a final concentration of 2×10^5 cells/mL, as determined with a hemocytometer. The cells were incubated for 15 minutes before use in the adhesion assay. Following the BSA blocking step, the solution was removed and the samples were rinsed three times with 1 mL of Tris·HCl buffer. Following this rinsing step, 2 mL of the cell solution was added to each well and the samples were incubated for 2 hours in a humidified atmosphere at 37° C and 5% CO_2. Three samples were prepared for each protein and substrate combination during each cell adhesion assay and the assay was repeated three times.

Cell Adhesion without BSA Blocking

The second cell adhesion assay was similar to the first, with one exception. In this assay, the substrates did not undergo a BSA blocking step. Instead, 24-well plates were blocked with 1 mg/mL heat denatured BSA for 30 minutes and rinsed three times with 1 mL of Tris·HCl buffer before the protein coated substrates were added. The substrates were rinsed three times with 1 mL of Tris·HCl buffer, followed by the addition of the cell solution. Two additional controls were added for these experiments as well. One control was prepared by exposing substrates to Tris·HCl buffer alone overnight at 4° C in a humidified atmosphere prior to use. The second control was BSA blocked wells that did not contain substrates, but were still exposed to cells. All of the other conditions remained the same as those described above and this assay was repeated four times.

Cell Binding Quantification

Following both cellular adhesion assays, the cell solution was removed from the well plates and the samples were rinsed three times with warm Tris·HCl buffer (37° C) to remove non-adherent cells. Following this rinse step, a Vybrant MTT cell proliferation assay kit was used to measure the number of adherent cells (Molecular Probes, Eugene, OR) following a scaled-up version of the recommended protocols. Briefly, 400 μL of phenol-red free α-MEM and 40 μL of 3-(4,5-dimethylthiazol-2-yl)-2,5-diphenyltetrazolium bromide (MTT) were added to each well. The well plates were incubated for 3 hours in a humidified atmosphere at 37° C and 5% CO_2. After the incubation period, 340 μL of the α-MEM/MTT solution was removed and 200 μL of dimethylsulfoxide (DMSO) was added. After 10 minutes, 150 μL of the solution from each well was transferred to a 96-well plate and the absorbance of light at 540 nm was measured using a Versamax tunable microplate reader with SoftmaxPro 3.1.1 software (Molecular Devices, Sunnyvale, CA). The results from individual experiments were normalized to each other based on the absorbance measured for control wells that underwent the MTT assay but were never exposed to cells. All other potential variations are accounted for in the experimental error shown as part of the results.

Data Analysis

The HAP elemental analysis and the absorbance measurement data is presented as the average of all of the measurements obtained and the error bars represent the standard error of the mean (SE). Sample results were analyzed using one-way analysis of variance (ANOVA) and they were considered statistically significant when they had a probability value less than 0.05 ($p<0.05$). Statistical analysis was performed using OriginPro 7.0 (OriginLab Corporation, MA).

Results

HAP Characterization

The formation of HAP from a SBF has been shown to result in the formation of a highly substituted mineral phase that more closely resembles native bone tissue than commercially available HAP, thus this method was used to produce HAP in this study.[43,44] HAP was formed on -COOH terminated SAMs for 1, 3, or 7 days from a SBF and then it was characterized with SEM and EDAX. The relative surface coverage and morphology of the HAP crystals can be seen in Figures 1a–c. In these images it can be seen that the surface coverage increases as the growth period is increased from 1 to 7 days and after 7 days there is no remaining uncovered Au. It appears that the size of the spherical HAP particles increases slightly from 1 day of growth to 3 days of growth, but they do not appear to grow further when the growth period is increased to 7 days. However, the underlying structure of the crystals is not different over the various growth periods when examined under higher magnification. Figure 1d shows a higher

magnification image of the spherical HAP particles after 7 days of growth and this image is representative of the HAP crystals that were found at all time points. In this figure, it can be seen that each of the spherical particles is composed of smaller plate-like pieces of HAP. Due to the possibility for slight variations in the crystal morphology between the different HAP growth periods, direct comparisons between the growth periods were not made in a quantitative manner in the cell studies that follow. However, qualitative observations based on this discussion were made in order to explain the trends that were seen.

The insets in Figures 1a–c are examples of the EDAX elemental analysis that was completed on each sample. This elemental analysis is summarized in Figure 2. The EDAX analysis of the mineral phase that was formed confirmed that a HAP-like crystal was nucleated onto the surface with traces of all of the elements provided in the SBF present in the samples over all of the growth periods. In Figure 2, it can be seen that the silicon and gold atomic percentages decrease noticeably as the growth period increases and this is an indicator of the relative surface coverage and thickness of the HAP above the gold coated glass cover slips. It can also be seen that the calcium and phosphate atomic percentages increase with the growth time. At the same time, the percentage of most of the other trace elements remains constant. Typically calcium phosphates are characterized by their Ca/P and O/Ca ratios. These were calculated and are summarized in Table 2 which shows these ratios for all three of the HAP growth periods as well as literature values for commercially available HAP and bone.[45] In this table it can be seen that the Ca/P ratio increases as the HAP growth period increases from 1 day to 7 days, while the O/Ca ratio decreases. Additionally, the ratios obtained for the HAP formed over 7 days closely resemble the literature values for both commercial HAP as well as bone, as shown in Table 2.

While the Ca/P ratios were lower than those found for commercial HAP and bone and the O/Ca ratios were higher for both the 1 day and 3 day HAP samples, it is believed that a similar mineral phase was formed over all of the growth time periods. The O/Ca ratio is clearly influenced by the elemental signatures from the underlying glass substrate at shorter HAP growth periods with reduced surface coverage. The relative levels of silicon and gold are noticeably higher on 1 day and 3 day HAP and these elements are only associated with the underlying gold coated glass cover slip. This reduced surface coverage results in an increased oxygen signal relative to the mineral specific elements (especially Ca). Furthermore, the morphology of the mineral that is formed over all of the time periods is similar as seen in the SEM images in Figure 1. The mineral forms spherical particles that are composed of smaller plate-like particles. The only differences between the growth time periods is in the relative levels of surface coverage and in the size of the spherical particles which appear to be slightly smaller on the 1 day growth samples. Finally, even if slightly different mineral phases are present from the different growth periods, the cell adhesion studies that follow confirmed that the cell binding levels were identical across all of the HAP control samples in the absence of adsorbed proteins.

OPN and BSP Isolation

The purity of the OPN and BSP used in this investigation is demonstrated by Figure 3. Figure 3a shows the impure, high molecular weight protein fraction ES1. This impure fraction can be compared to the protein bands obtained for purified OPN and BSP, which are shown in Figure 3b. Neither protein band was seen following staining with Coomassie brilliant blue, as these highly acidic, phosphorylated [0]proteins react poorly or do not react at all with Coomassie brilliant blue.[46] The identities of OPN and BSP were further confirmed by Western immunoblots using antibodies specific to OPN and BSP, respectively (data not shown).

Protein Adsorption Isotherms

Radiolabeled adsorption isotherms were obtained for both OPN and BSP by determining the adsorbed amount of protein from different solution concentrations on HAP grown for 14 days. This growth period was selected in order to ensure that the surface was fully coated in HAP. This was done to minimize the protein adsorption to the background -COOH terminated SAM in order to characterize the adsorption profiles that occur because of the specific binding interaction between the proteins and HAP. The adsorbed amount of protein was calculated based on the specific radioactivity of the protein solutions before adsorption and the cpm of each of the samples following the adsorption and rinsing steps. The resulting adsorption isotherms are shown in Figure 4. The isotherms for the two proteins were compared to determine the solution concentrations of OPN and BSP that result in equal amounts of protein adsorbed to the HAP, and these concentrations are indicated with dotted lines. Identical surface concentrations of adsorbed proteins allow for a direct comparison of the cell binding behaviors of these two proteins on the substrates examined using cell adhesion assays. Specifically, 50 μg/mL of OPN and 35 μg/mL of BSP were used with all of the substrates for the cellular assays. These conditions resulted in approximately 1.4 ng/mm^2 of adsorbed protein on each of the substrates examined.

The protein adsorption isotherms indicate that HAP has the capacity to bind significantly more BSP than OPN as seen in Figure 4. These findings are in close agreement with recent protein chemistry data that shows that BSP is bound more tightly to the mineral phase of bone and dentin. In those experiments, it was determined that large amounts of OPN can be extracted by GdmCl alone (without EDTA) whereas significant amounts of BSP can only be extracted when 0.5 M EDTA is present in the extraction solution (Qin *et al*, unpublished observations). In this study, OPN is seen to have a typical Langmuir adsorption isotherm profile, with an adsorption plateau at 1.4–1.5 ng/mm^2. At the same time, BSP has a largely linear adsorption isotherm profile over the range of solution concentrations that were examined. It is possible that these differences may be related to differences in the amino acid sequences believed to mediate the HAP binding properties of the two proteins (poly-aspartic acid versus poly-glutamic acid), but a detailed examination of this is beyond the scope of the current study.[7,47] It is also interesting to note that the adsorption profiles for these two proteins are the exact opposite of those seen in related studies with collagen type I.[34,36] In these previous studies, OPN was shown to have a largely linear adsorption profile while BSP was shown to plateau when the adsorption solution concentration reached 50 μg/mL. When those two studies are taken in conjunction with this one, they may indicate more about the roles that these two proteins play in bone interfacial zones.

Cell Adhesion with BSA Blocking

The first cell adhesion assay was completed by soaking protein coated substrates in heat denatured BSA prior to completing the cell binding studies to block non-specific cell binding to the background substrate. The cell binding was measured on four surfaces, -COOH terminated SAMs (or 0 days of HAP growth), 1 day HAP, 3 day HAP, and 7 day HAP, in the presence of one of the three proteins, BSA, OPN, or BSP, with an MTT cell binding assay kit. The results are summarized in Figure 5. In this figure it can be seen that on -COOH terminated SAMs there were statistically significant differences in the cell binding between all three proteins. The highest cell binding levels were obtained on surfaces with adsorbed BSP. OPN coated surfaces had the next highest cell binding and BSA coated surfaces had the least amount of cell binding. On 1 day HAP, BSP coated surfaces again showed the highest levels of cell binding followed by BSA and OPN coated surfaces, respectively. The only statistically significant difference on this substrate was between the OPN and BSP coated surfaces. On 3 day HAP substrates, the greatest levels of cell binding were obtained on BSA coated surfaces. BSP coated surfaces had a very similar amount of cell binding and both had statistically greater

cell binding than that on the OPN coated substrate. Finally, on HAP grown for 7 days, the greatest cell binding was seen in the presence of BSA, while BSP and OPN had similar levels of cell binding, with a slight preference for BSP. The only statistically significant difference on this substrate was between the BSA and OPN coated surfaces.

These results suggest that BSP has a more favorable orientation or conformation than OPN for cell binding when they are specifically bound to HAP. This is supported by the fact that BSP has statistically greater levels of cell binding on HAP grown for 0, 1, and 3 days. Interestingly, this is the opposite behavior for what was seen in the previous study utilizing collagen, where OPN was shown to have statistically greater levels of cell binding.[34] However, these results appear to be influenced by the adsorbed BSA, based on the high levels of cell binding to HAP with only adsorbed BSA. At the same time, the influence on the cell binding by BSA should be similar between these two surfaces. The adsorption isotherms were used to identify conditions that result in identical amounts of adsorbed protein (mass per area) and OPN and BSP are very similar in size and molecular weight. This should result in very similar levels of surface coverage by OPN and BSP resulting in similar amounts of adsorbed BSA. One exception would occur if BSA has a specific binding interaction with HAP that directly competes with one of the other two proteins, but this is not expected because no HAP binding sites have been identified in the BSA amino acid sequence. This is examined in more detail in the cell adhesion assay without BSA blocking as discussed below. Previously, OPN was shown to have a favorable orientation for MC3T3-E1 cell binding when it was specifically bound to collagen, while BSP was shown to have more conformational flexibility around its RGD cell binding moiety.[34] The results obtained in this study support the previous conclusion that the orientation of OPN can be controlled. However, the specific binding interaction between HAP and OPN leads to a negative orientation for cell binding rather than the positive orientation seen in the previous study. Additionally, it is possible that conformational flexibility around the RGD moiety in BSP leads to the higher levels of cell binding seen in this study.

It should also be noted that the cell binding on HAP grown for 7 days decreases as compared with the cell binding to HAP grown for both 1 and 3 days in the presence of adsorbed proteins. This decrease in the number of bound cells occurs for all three of the proteins indicating that it is likely to be caused by surface characteristics rather than the proteins. It is suspected that the increased surface roughness reduces the overall number of adherent cells by limiting the number cell surface contacts. The relative surface roughness can be gauged qualitatively in the SEM images of the HAP in Figure 1a–c.

Cell Adhesion without BSA Blocking

Because high levels of cell binding were obtained in the first cell binding assay in the presence of BSA alone, the adhesion assays were redone with substrates that did not undergo a BSA soak to block non-specific cell adhesion. This would allow for the analysis of the role that BSA played in the cell binding to both OPN and BSP coated surfaces. As an added control, substrates without any adsorbed proteins were included in these cell studies and all of these results are summarized in Figure 6. On -COOH terminated SAM surfaces there were statistically significant differences in the cell binding between the BSA coated surface and the other two protein cases as well as the substrate with no adsorbed proteins. The cell binding levels followed the following trend: BSP > OPN > Tris·HCl buffer > BSA. However, only the BSA cases showed statistically significant differences from the others. On 1 day HAP the cell binding was statistically greater on the BSA coated surface as compared to the surfaces with the other two proteins and the surface with no adsorbed protein. The second highest cell binding was seen on BSP coated HAP, followed by OPN and Tris·HCl buffer. There was a statistical difference in the cell binding between the BSP coated surface and the surface without any adsorbed protein indicating improved cell binding on this substrate. The only statistical differences that were

observed on the 3 day HAP were again between the BSA coated substrates and the other three cases. While there were no statistically significant differences between the other three cases, there was a slight preference for cell binding to BSP over OPN and the no protein case. On HAP grown for 7 days it was observed that the only significant differences were again between the BSA coated surface and the other three cases. However, this time the statistical significance was only at a 95% confidence level ($p<0.05$), unlike the three previous substrates where there was a significance at a 99% confidence level ($p<0.01$). Finally, the cell binding to BSA blocked TCPS wells was measured and was found to have an $A_{540\ nm}$ of 0.010 ± 0.003, indicating that there is minimal cell binding to the background well plate and that the cell binding occurs on the HAP substrates.

These results support the earlier conclusion that OPN has a negative orientation for cell binding when specifically bound to HAP. This is based on the fact that OPN does not improve the cell binding to HAP beyond the background cell binding that occurs to HAP in the absence of adsorbed proteins. This would suggest that the RGD cell binding moiety in OPN is unavailable for interactions with the MC3T3-E1 cells during the cell adhesion assay. Additionally, BSP again has slightly higher cell binding levels than OPN, although these differences were not statistically significant. BSP also had statistically greater levels of cell binding than the HAP control on the 1 day HAP samples.

Figure 6 also indicates where there were statistically significant differences between the BSA soaked and unsoaked substrates, indicating where this soaking step influenced the cellular binding. Differences were seen at a 95% confidence level for BSA on both the -COOH substrate and the 1 day HAP samples. Differences were also seen in the BSP cases on both 1 day and 3 day HAP and for OPN on the 3 day HAP. This indicates that BSA influenced the cell binding on a number of substrates and required a closer examination. It should be noted that there were no differences in the cell binding to HAP grown for 7 days between the surfaces with and without BSA blocking for all three proteins. Furthermore, the number of bound cells on this surface (without blocking) is again lower than that seen for both the 1 day and 3 day HAP surfaces. This trend was similar to that seen in Figure 5 and it supports the earlier hypothesis that the overall surface roughness plays a greater role in the cellular binding to this substrate than the presence of the proteins.

BSA Cell Adhesion Assay

BSA was seen to have significantly greater cell binding on all of the HAP surfaces as compared to the other two proteins in the second cell binding assay. In order to probe this phenomenon, a cell binding assay was completed on 3 day HAP to examine the influence that the BSA solution concentration had on the subsequent cell binding. The results of this assay can be seen in Figure 7. In this figure it can be seen that there is an increasing level of cell adhesion on 3 day HAP as the concentration of BSA is increased from 0 mg/mL to 1.0 mg/mL. A statistical analysis was not performed on these results due to the limited sample size.

These results were unexpected because previous studies have shown that heat denatured BSA is an effective protein for preventing non-specific cell binding to many substrates.[30,33,34,36] In previous studies with MC3T3-E1 cells, it was shown that heat denatured BSA effectively prevents cell binding to TCPS and this was confirmed in this study. Additionally, in both cell binding assays, the lowest amount of cell binding was seen on -COOH terminated SAMs (0 days of HAP growth) with adsorbed BSA. These two results indicate that BSA is effective at blocking MC3T3-E1 cell binding to some substrates. However, Figure 6 shows that the HAP samples with adsorbed BSA have a significantly greater number of bound cells as compared to all of the other HAP samples both with and without adsorbed protein. This was confirmed in Figure 7 where increasing concentrations of BSA led to increasing levels of cell binding to 3 day HAP in a dose dependant manner.

Discussion

Based on the results obtained in this study and in our previous studies,[34,36] we have developed a hypothesis regarding the relative locations of the collagen binding domain, the HAP binding domain, and the RGD sequence in both OPN and BSP. Based on the fact that OPN was shown to have a positive orientation for cell binding when specifically bound to collagen I and a negative orientation for cell binding when specifically bound to HAP, it is likely that the RGD sequence is located near the HAP binding domain in the three dimensional structure of OPN. This is shown schematically in Figure 8. At the same time, BSP was seen to promote a slight improvement in the cell binding in both systems, but this was attributed to conformational flexibility surrounding its RGD region. It is likely that the RGD sequence is not located near either one of the specific binding domains for HAP or collagen. The collagen binding property of BSP has been shown to be dependant upon amino acids 21-42 [48] which are near both of the HAP binding domains at the N-terminus of the protein. At the same time, the RGD sequence is located at the C-terminus end of the protein.[20] The hypothesized locations of these three regions of BSP, relative to each other, are also shown schematically in Figure 8.

Interestingly, the biggest impact on the MC3T3-E1 cell binding to HAP was found on substrates with adsorbed BSA. This was unexpected because unlike OPN and BSP, BSA does not have a known cell binding moiety. There are two possible explanations for the observation that BSA improves the cell binding in these studies: 1) it is possible that an impurity in the albumin is influencing the cell binding or 2) that the albumin is influencing the adhesion or proliferation activity of the bound cells. While the first possibility can not be completely ruled out, it seems unlikely because a similar cell response was seen on HAP when other commercially available albumins were adsorbed to the surface (data not shown). Additionally, BSA was shown to effectively block cell binding on both TCPS and -COOH terminated SAMs in this study. The second possibility is a more likely explanation for the results that were obtained. The MTT assay that was used to measure cell binding is designed to recognize the mitochondrial activity of cells. In this assay MTT is taken up by living cells and processed into formazan crystals. The formazan is released from the cells with the addition of DMSO and the level of formazan is measured directly by absorbance. As a result, this assay can be used to measure the amount of bound cells, but it is actually a probe of the mitochondrial activity of the cells that are present. A series of studies by Yamaguchi and colleagues have suggested that albumin is released by osteoblast cells present in fracture healing sites and this excess albumin increases the proliferation state of the surrounding cells.[49–51] In one of these studies, Ishida and Yamaguchi showed that supplementing a standard culture medium with varying amounts of BSA led to a significant increase in the number of MC3T3-E1 cells present after 24, 48, and 72 hours of culture in a dose dependent manner.[49] A similar trend was seen in the number of cells present in this study after only 5 total hours of cell culture (2 hours of adhesion and 3 hours of MTT uptake) as shown in Figure 7. However, in this study the surface was exposed to BSA overnight, followed by three rinsing steps, prior to cell seeding. In the study by Ishida and Yamaguchi the BSA was included as a supplement to the culture medium and was present in both an adsorbed state and in solution throughout the studies. The results of this study would indicate that it is the adsorption state of the BSA that influences the activity or amount of adherent cells rather that its presence in solution alone. In previous work by Webster *et al*, it was found that the adsorption of albumin to the surface of conventional and nanophase ceramics (including HAP) did not improve the osteoblast binding.[11] However, in that study the maximum concentration of albumin that the surfaces were exposed to was 5 μg/mL. In this study it was found that there is no measurable influence on the adhesion of cells until the BSA exposure concentration reached 0.25 mg/mL (or 250 μg/mL), as shown in Figure 7. Furthermore, in a recent study by Kim *et al* it was found that a surface modification with 2% BSA led to significant improvements in the attachment, proliferation, and differentiation of MG-63 osteoblast-like cells to a HAP based scaffold.[52] These results, taken in conjunction with the

results of this study suggest that BSA may have a specific binding interaction with HAP that results in an improvement in the bioactive state for osteoblast cells with regards to adhesion and proliferation. However, this improvement only occurs when the surface concentration of BSA is above a certain threshold.

Conclusions

The orientation and conformation of OPN and BSP adsorbed to HAP were examined in this work. It was determined that OPN has a negative orientation for cell binding when specifically bound to HAP. BSP had slightly higher levels of cell binding as compared to OPN, but not to a statistically significant level. BSP did however improve the cell binding to the background HAP for one of the growth periods examined. Furthermore, a hypothesis was presented which localized the collagen I and HAP binding domains relative to the RGD moiety, for both OPN and BSP. However, the improvement in the number of bound cells for substrates with adsorbed BSP was overshadowed by the improvement seen for substrates with adsorbed heat denatured BSA. The presence of BSA led to the maximal cell binding on all of the HAP substrates examined in this study. It was concluded that BSA influences the adhesion and proliferation of osteoblast cells to HAP and based on these results it might be possible to develop better HAP-based biomaterials through the incorporation of albumin into the mineral matrix to improve the cell adhesion and proliferation capacity.

Acknowledgements

We would like to acknowledge Drs. L. Cao and T. Horbett at the University of Washington for their assistance with the radiolabeling studies and Dr. F. Baneyx at the University of Washington for the use of a microplate reader in his group. The SEM and EDAX analyses were performed at the University of Washington Center for Nanotechnology, one of the twelve nodes of the National Nanotechnology Infrastructure Network supported by the National Science Foundation. MTB was supported during a portion of this work by a University of Washington Center for Nanotechnology IGERT Fellowship. This work was also supported by the National Science Foundation through CTS-0092699 (CAREER Award) and EEC-9529161 (UWEB) and the National Institute of Health through DE005092 (CQ).

References

1. LeGeros RZ. Properties of Osteoconductive Biomaterials: Calcium Phosphates. Clinical Orthopaedics and Related Research 2002;395(1):81–98. [PubMed: 11937868]
2. Chou Y, Huang W, Dunn JCY, Miller TA, Wu BM. The Effect of Biomimetic Apatite Structure on Osteoblast Viability, Proliferation, and Gene Expression. Biomaterials 2005;26(3):285–295. [PubMed: 15262470]
3. Hofmann A, Konrad L, Gotzen L, Printz H, Ramaswamy A, Hofmann C. Bioengineered Human Bone Tissue Using Autogenous Osteoblasts Cultured on Different Biomatrices. Journal of Biomedical Materials Research 2003;67A(1):191–199. [PubMed: 14517876]
4. Hong JY, Kim YJ, Lee HW, Lee WK, Ko JS, Kim HM. Osteoblastic Cell Response to Thin Film of Poorly Crystalline Calcium Phosphate Apatite Formed at Low Temperatures. Biomaterials 2003;24 (18):2977–2984. [PubMed: 12895569]
5. Inoue M, LeGeros RZ, Inoue M, Tsujigiwa H, Nagatsuka H, Yamamoto T, Nagai N. In Vitro Response of Osteoblast-Like and Odontoblast-Like Cells to Unsubstituted and Substituted Apatites. Journal of Biomedical Materials Research 2004;70A(4):585–593. [PubMed: 15307163]
6. Ogata K, Imazato S, Ehara A, Ebisu S, Kinomoto Y, Nakano T, Umakoshi Y. Comparison of Osteoblast Responses to Hydroxyapatite and Hydroxyapatite/Soluble Calcium Phosphate Composites. Journal of Biomedical Materials Research 2005;72A(2):127–135. [PubMed: 15625683]
7. Addadi L, Weiner S. Interactions Between Acidic Proteins and Crystals: Stereochemical Requirements in Biomineralization. Proceedings of the National Academy of Sciences 1985;82(12):4110–4114.
8. Gilbert M, Giachelli CM, Stayton PS. Biomimetic Peptides that Engage Specific integrin Dependant Signaling Pathways and Bind to Calcium Phosphate Surfaces. Journal of Biomedical Materials Research, Part A 2003;67A(1):69–77. [PubMed: 14517863]

9. Goldberg HA, Warner KJ, Li MC, Hunter GK. Binding of Bone Sialoprotein, Osteopontin and Synthetic Polypeptides to Hydroxyapatite. Connective Tissue Research 2001;42(1):25–37. [PubMed: 11696986]
10. Krout A, Wen HH, Hippensteel E, Li P. A Hybrid Coating of Biomimetic Apatite and Osteocalcin. The Journal of Biomedical Materials Research 2005;73A(1):377–387.
11. Webster TJ, Ergun C, Doremus RH, Siegel RW, Bizios R. Specific Proteins Mediate Enhanced Osteoblast Adhesion on Nanophase Ceramics. Journal of Biomedical Materials Research 2000;51 (3):475–483. [PubMed: 10880091]
12. Gokhale, JA.; Boskey, AL.; Robey, PG. Chapter 4: The Biochemistry of Bone. In: Marcus, R.; Feldman, D.; Kelsey, J., editors. Osteoporosis. San Diego: Academic Press; 2001. p. 107-188.
13. Roach HI. Why Does Bone Matrix Contain Non-Collagenous Proteins? The Possible Roles of Osteocalcin, Osteonectin, Osteopontin, and Bone Sialoprotein in Bone Mineralization and Resorption. Cell Biology International 1994;18(6):617–628. [PubMed: 8075622]
14. Veis A. Mineral-Matrix Interactions in Bone and Dentin. Journal of Bone and Mineral Research 1993;8(S2):S493–S497. [PubMed: 8122518]
15. Nanci A. Content and Distribution of Noncollagenous Matrix Proteins in Bone and Cementum: Relationship to Speed of Formation and Collagen Packing Density. Journal of Structural Biology 1999;126(3):256–269. [PubMed: 10441531]
16. Puleo DA, Nanci A. Understanding and Controlling the Bone-Implant Interface. Biomaterials 1999;20 (23–24):2311–2321. [PubMed: 10614937]
17. Fisher LW, Torchia DA, Fohr B, Young MF, Fedarko NS. Flexible Structures of SIBLING Proteins, Bone Sialoprotein, and Osteopontin. Biochemical and Biophysical Research Communications 2001;280(2):460–465. [PubMed: 11162539]
18. Butler, WT.; Ridall, AL.; McKee, MD. Chapter 13: Osteopontin. In: Bilezikian, JP.; Raisz, LG.; Rodan, GA., editors. Principles of Bone Biology. San Diego: Academic Press; 1996. p. 167-182.
19. Sodek J, Ganss B, McKee MD. Osteopontin. Critical Reviews in Oral Biology and Medicine 2000;11 (3):279–303. [PubMed: 11021631]
20. Ganss B, Kim RH, Sodek J. Bone Sialoprotein. Critical Reviews in Oral Biology and Medicine 1999;10(1):79–98. [PubMed: 10759428]
21. Giachelli CM, Steitz S. Osteopontin: A Versatile Regulator of Inflammation and Biomineralization. Matrix Biology 2000;19(7):615–622. [PubMed: 11102750]
22. Gorski JP. Is All Bone the Same? Distinctive Distributions and Properties of Non-collagenous Matrix Proteins in Lamellar vs. Woven Bone Imply the Existence of Different Underlying Osteogenic Mechanisms. Critical Reviews in Oral Biology and Medicine 1998;9(2):201–223. [PubMed: 9603236]
23. Mazzali M, Kipari T, Ophascharoensuk V, Wesson JA, Johnson R, Hughes J. Osteopontin - A Molecule for All Seasons. QJM-An International Journal of Medicine 2002;95(1):3–13. [PubMed: 11834767]
24. Siebers MC, terBrugge PJ, Walboomers XF, Jansen JA. Integrins as Linker Proteins Between Osteoblasts and Bone Replacing Materials. A Critical Review Biomaterials 2005;26(2):137–146.
25. Chen Y, Bal BS, Gorski JP. Calcium and Collagen Binding Properties of Osteoponin, Bone Sialoprotein, and Bone Acidic Glycoprotein-75 from Bone. The Journal of Biological Chemistry 1992;267(34):24871–24878. [PubMed: 1447223]
26. Fujisawa R, Kuboki Y. Affinity of Bone Sialoprotein and Several Other Bone and Dentin Acidic Proteins to Collagen Fibrils. Calcified Tissue International 1992;51(6):438–442. [PubMed: 1451011]
27. Castner DG, Ratner BD. Biomedical Surface Science: Foundations to Frontiers. Surface Science 2002;500(1–3):28–60.
28. Tirrell M, Kokkoli E, Biesalski M. The Role of Surface Science in Bioengineered Materials. Surface Science 2002;500(1–3):61–83.
29. Wilson CJ, Clegg RE, Leavesley DI, Pearcy MJ. Mediation of Biomaterial-Cell Interactions by Adsorbed Proteins: A Review. Tissue Engineering 2005;11(12):1–18. [PubMed: 15738657]
30. Liu L, Chen S, Giachelli CM, Ratner BD, Jiang S. Controlling Osteopontin Orientation on Surfaces to Modulate Endothelial Cell Adhesion. Journal of Biomedical Materials Research 2005;74A(1):23–31. [PubMed: 15920735]

31. Wang H, Castner DG, Ratner BD, Jiang S. Probing the Orientation of Surface Immobilized Immunoglobulin G by Time-of-Flight Secondary Ion Mass Spectrometry. Langmuir 2004;20(5): 1877–1887. [PubMed: 15801458]
32. Bernards MT, Jiang S. pH Induced Conformation Changes of Adsorbed Vitronectin Maximize Its Bovine Aortic Endothelial Cell Binding Ability. Journal of Biomedical Materials Research Part A. Accepted 2007
33. Wang H, He Y, Ratner BD, Jiang S. Modulating Cell Adhesion and Spreading by Control of $FnIII_{7-10}$ Orientation on Charged Self-Assembled Monolayers (SAMs) of Alkanethiolates. Journal of Biomedical Materials Research 2006;77A(4):672–678. [PubMed: 16514600]
34. Bernards MT, Qin C, Ratner BD, Jiang S. Adhesion of MC3T3-E1 Cells to Bone Sialoprotein and Bone Osteopontin Specifically Bound to Collagen I. Journal of Biomedical Materials Research Part A. Accepted 2007
35. Calonder D, Matthew HWT, Tassel PRV. Adsorbed Layers of Oriented Fibronectin: A Strategy to Control Cell-Surface Interactions. Journal of Biomedical Materials Research, Part A 2005;75A(2): 316–323. [PubMed: 16059890]
36. Liu L, Qin C, Butler WT, Ratner BD, Jiang S. Controlling the Orientation of Bone Osteopontin via its Specific Binding with Collagen I to Modulate Osteoblast Adhesion. Journal of Biomedical Materials Research, Part A 2007;80A(1):102–110. [PubMed: 16960829]
37. Oyane A, Onuma K, Ito A, Kim H, Kokubo T, Nakamura T. Formation and Growth of Clusters in Conventional and New Kinds of Simulated Body Fluids. Journal of Biomedical Materials Research 2003;64A(2):339–348. [PubMed: 12522821]
38. Wang H, Chen S, Li L, Jiang S. Improved Method for the Preparation of Carboxylic Acid and Amine Terminated Self-Assembled Monolayers of Alkanethiolates. Langmuir 2005;21(7):2633–2636. [PubMed: 15779923]
39. Prince CW, Oosawa T, Butler WT, Tomana M, Bhown AS, Bhown M, Schrohenloher RE. Isolation, Characterization, and Biosynthesis of a Phosphorylated Glycoprotein from Rat Bone. Journal of Biological Chemistry 1987;262(6):2900–2907. [PubMed: 3469201]
40. Qin C, Brunn JC, Jones J, George A, Ramachadran A, Gorski JP, Butler WT. A Comparative Study of Sialic Acid-rich Proteins in Rat Bone and Dentin. European Journal of Oral Sciences 2001;109 (2):133–141. [PubMed: 11347657]
41. Horbett, TA. Techniques of Biocompatibility Testing. Boca Raton: CRC Press, Inc.; 1986.
42. Freitas F, Jeschke M, Majstorovic I, Mueller DR, Schindler P, Voshol H, Oostrum JV, Susa M. Fluoroaluminate Stimulates Phosphorylation of p130 Cas and Fak and Increases Attachment and Spreading of Preosteoblastic MC3T3-E1 Cells. Bone 2002;30(1):99–108. [PubMed: 11792571]
43. Landi E, Tampieri A, Celotti G, Langenati R, Sandri M, Sprio S. Nucleation of Biomimetic Apatite in Synthetic Body Fluids: Dense and Porous Scaffold Development. Biomaterials 2005;26(16):2835–2845. [PubMed: 15603779]
44. Sato K, Kumagai Y, Tanaka J. Apatite Formation on Organic Monolayers in Simulated Body Environment. Journal of Biomedical Materials Research 2000;50(1):16–20. [PubMed: 10644958]
45. Lu HB, Campbell CT, Graham DJ, Ratner BD. Surface Characterization of Hydroxyapatite and Related Calcium Phosphates by XPS and ToF-SIMS. Analytical Chemistry 2000;72(13):2886–2894. [PubMed: 10905323]
46. Myers JM, Veis A, Sabsay B, Wheeler AP. A Method for Enhancing the Sensitivity and Stability of Stains-All for Phosphoproteins Separated in Sodium Dodecyl Sulfate-Polyacrylamide Gels. Analytical Biochemistry 1996;240(2):300–302. [PubMed: 8811925]
47. Fujisawa R, Kuboki Y. Preferential Adsorption of Dentin and Bone Acidic Proteins on the (100) Face of Hydroxyapatite Crystals. Biochimica et Biophysica Acta 1991;1075(1):56–60. [PubMed: 1654109]
48. Tye CE, Hunter GK, Goldberg HA. Identification of the Type I Collagen-Binding Domain of Bone Sialoprotein and Characterization of the Mechanism of Interaction. The Journal of Biological Chemistry 2005;280(14):13487–13492. [PubMed: 15703183]
49. Ishida K, Yamaguchi M. Role of Albumin in Osteoblastic Cells: Enhancement of Cell Proliferation and Suppression of Alkaline Phosphatase Activity. International Journal of Molecular Medicine 2004;14(6):1077–1081. [PubMed: 15547677]

50. Ishida K, Yamaguchi M. Albumin Regulates Runx2 and α1 (I) Collagen mRNA Expression in Osteoblastic Cells: Comparison with Insulin-Like Growth Factor-1. International Journal of Molecular Medicine 2005;16(4):689–694. [PubMed: 16142406]

51. Yamaguchi M, Igarashi A, Misawa H, Tsurusaki Y. Enhancement of Albumin Expression in Bone Tissues with Healing Rat Fractures. Journal of Cellular Biochemistry 2003;89(2):356–363. [PubMed: 12704798]

52. Kim YU, LeGeros RZ, Kim KN, Kim KM, Lee YK. Effect of Calcium Phosphate Glass on Proliferation and Differentiation of MG-63 Cells in HA Scaffolds. Materials Science Forum 2007;539–543(1):731–736.

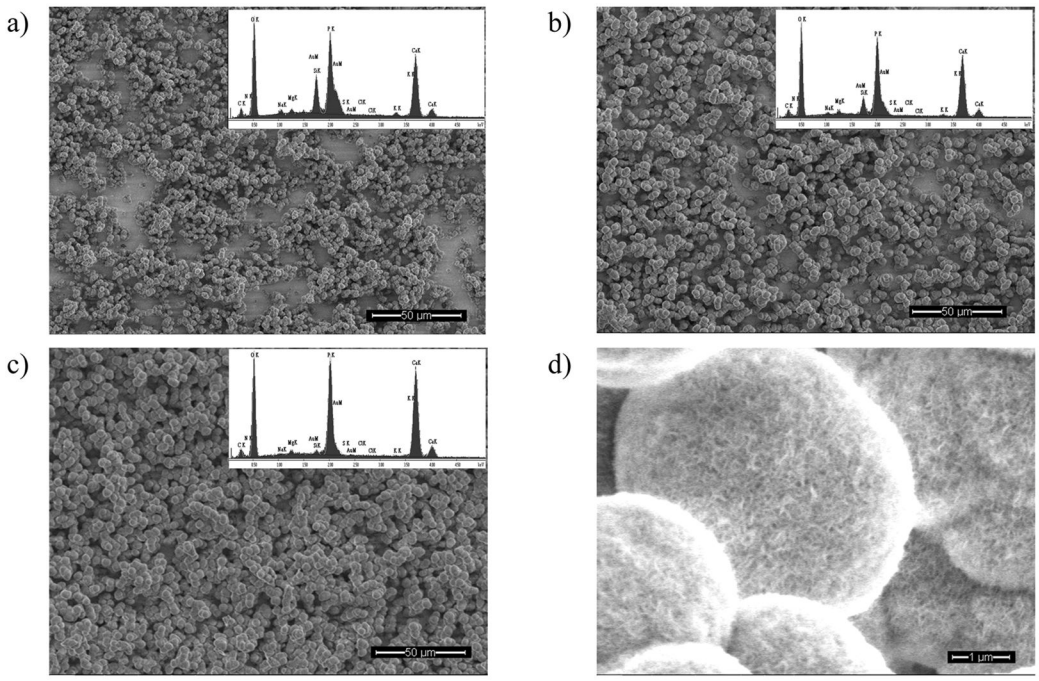

Figure 1.
SEM images of HAP grown for (a) 1 day, (b) 3 days, and (c) 7 days from SBF onto -COOH terminated SAMs. The magnified image (d) was taken from HAP grown for 7 days, but it is representative of the morphology of the HAP grown over each of the different time periods. The inset images are representative EDAX plots for each of the samples.

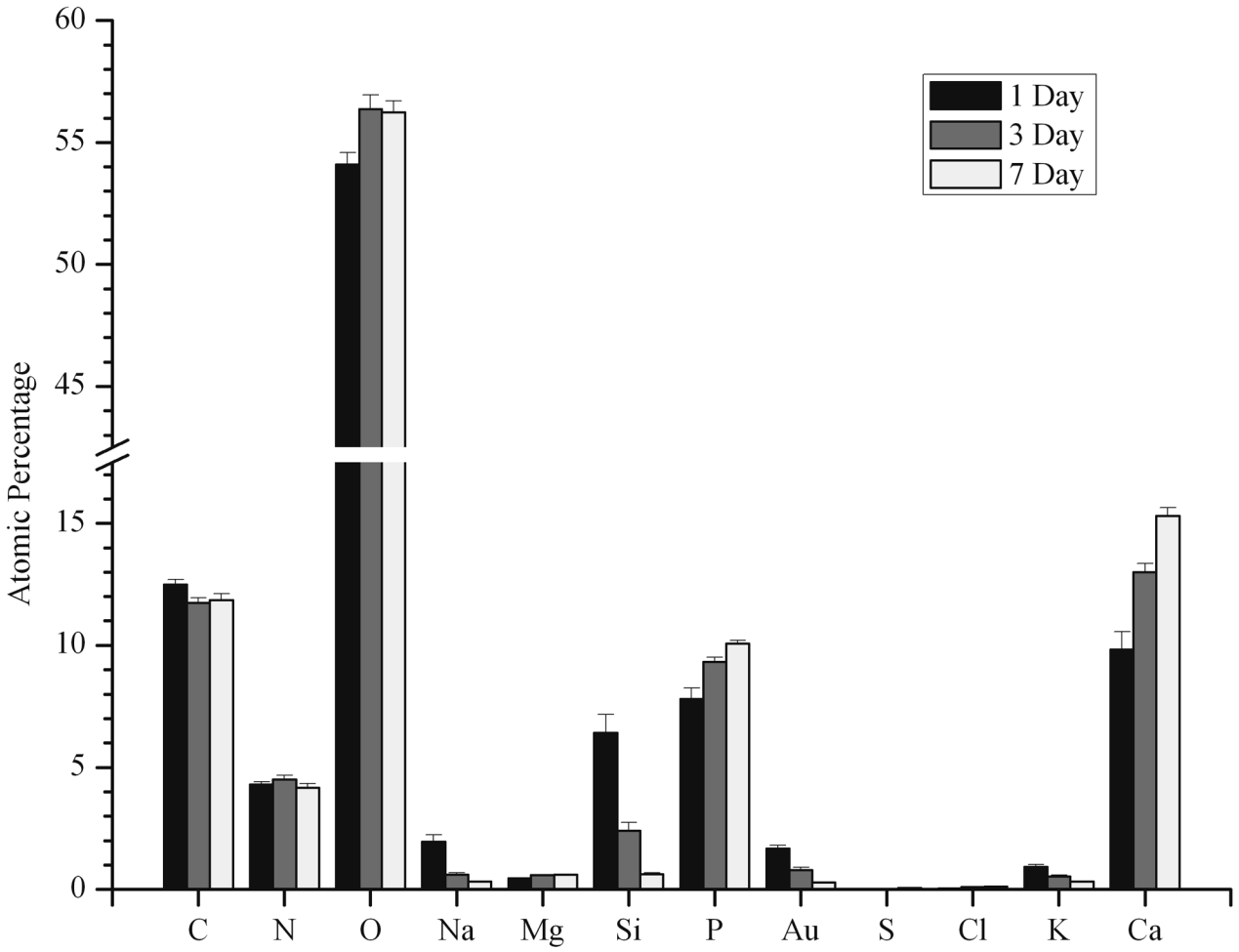

Figure 2.
Elemental composition of HAP grown from SBF onto -COOH terminated SAMs for 1, 3, and 7 days as measured by EDAX. The data is presented as the mean ± SE collected from three spots on each of four samples (n = 12) for each growth time period.

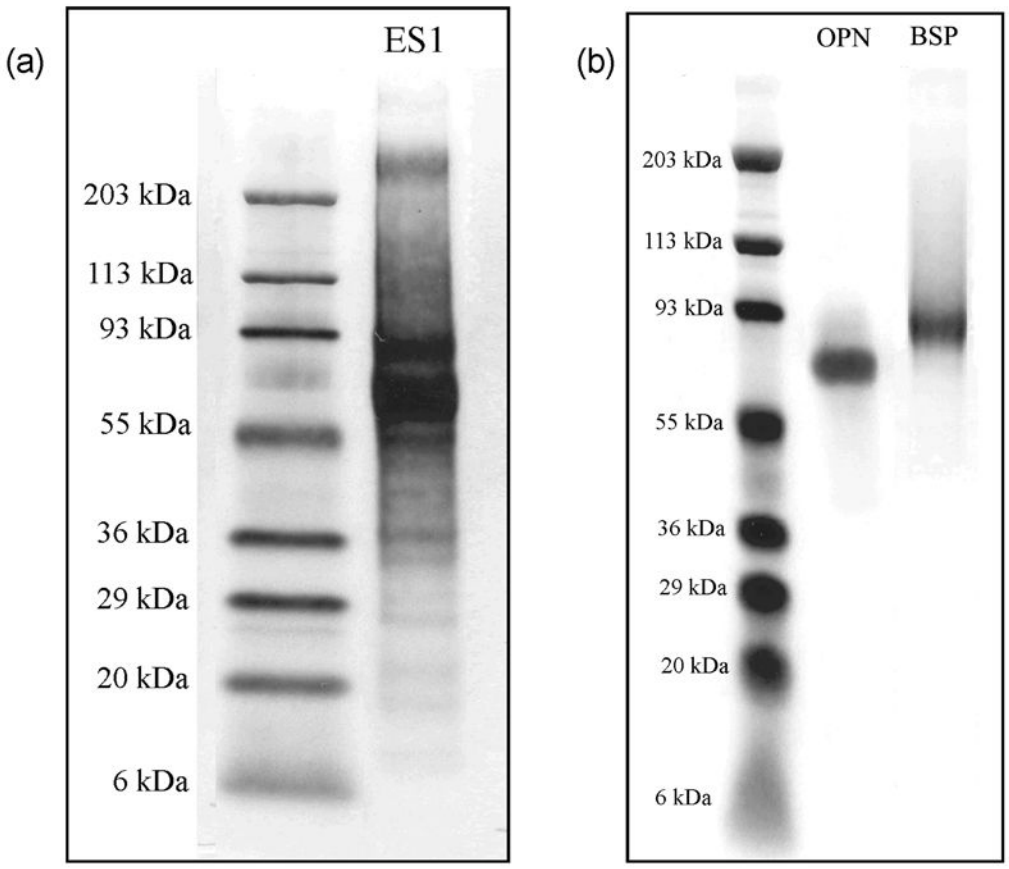

Figure 3.

SDS-PAGE and Stains-All staining of protein fractions: (a) Stains-All staining of the impure, high molecular weight protein fraction (ES1), obtained after the removal of smaller molecular weight bone proteins; (b) Stains-All staining of OPN (Lane 2) and BSP (Lane 3). Lane 1 in both (a) and (b) was loaded with molecular weight standards. The lanes were loaded with 15 μg of ES1 and 6 μg of OPN and BSP, respectively.

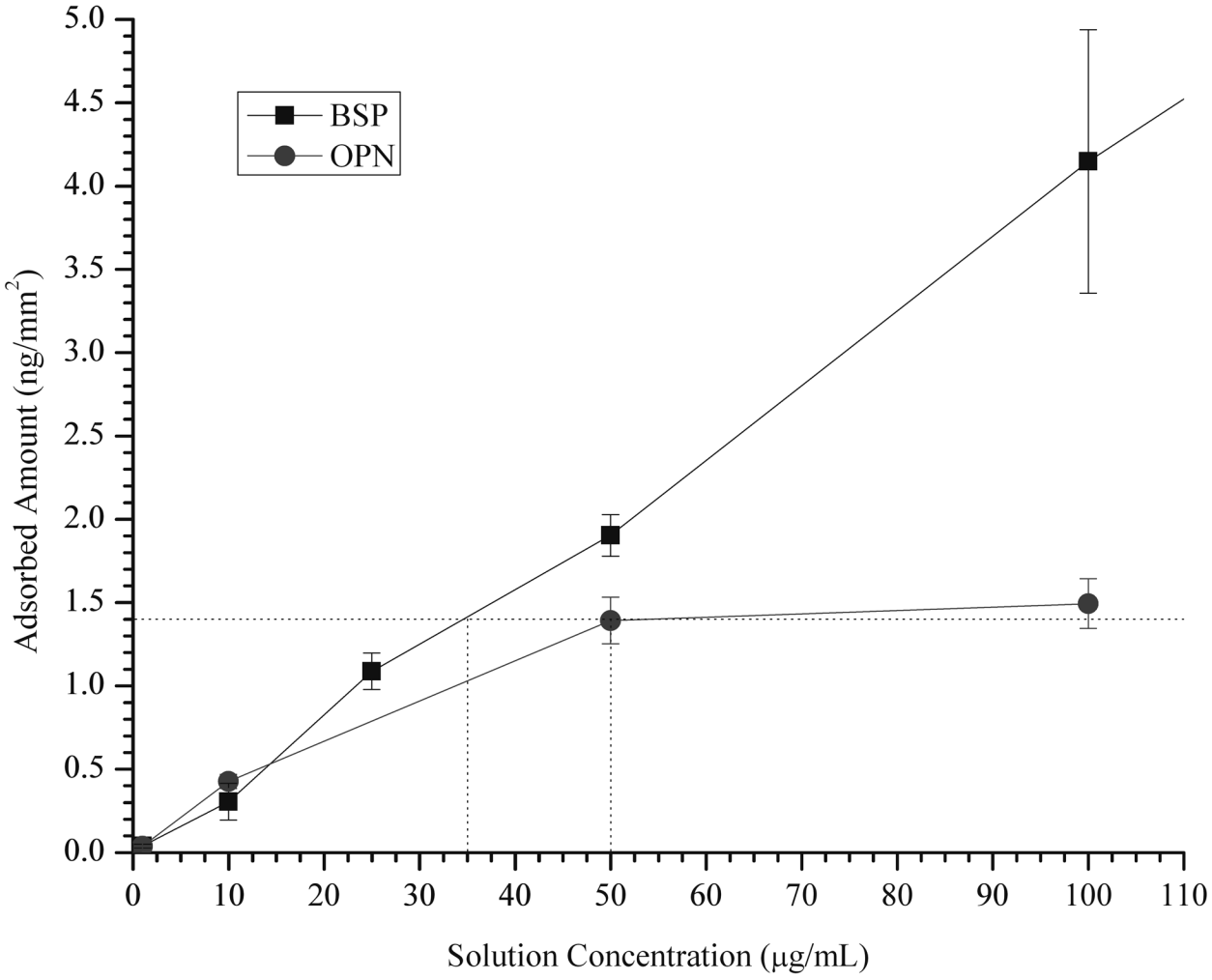

Figure 4.
^{125}I radiolabel adsorption isotherms for BSP (squares) and OPN (circles) on HAP grown for two weeks. The dotted lines represent the protein exposure concentrations used for the cell adhesion assays.

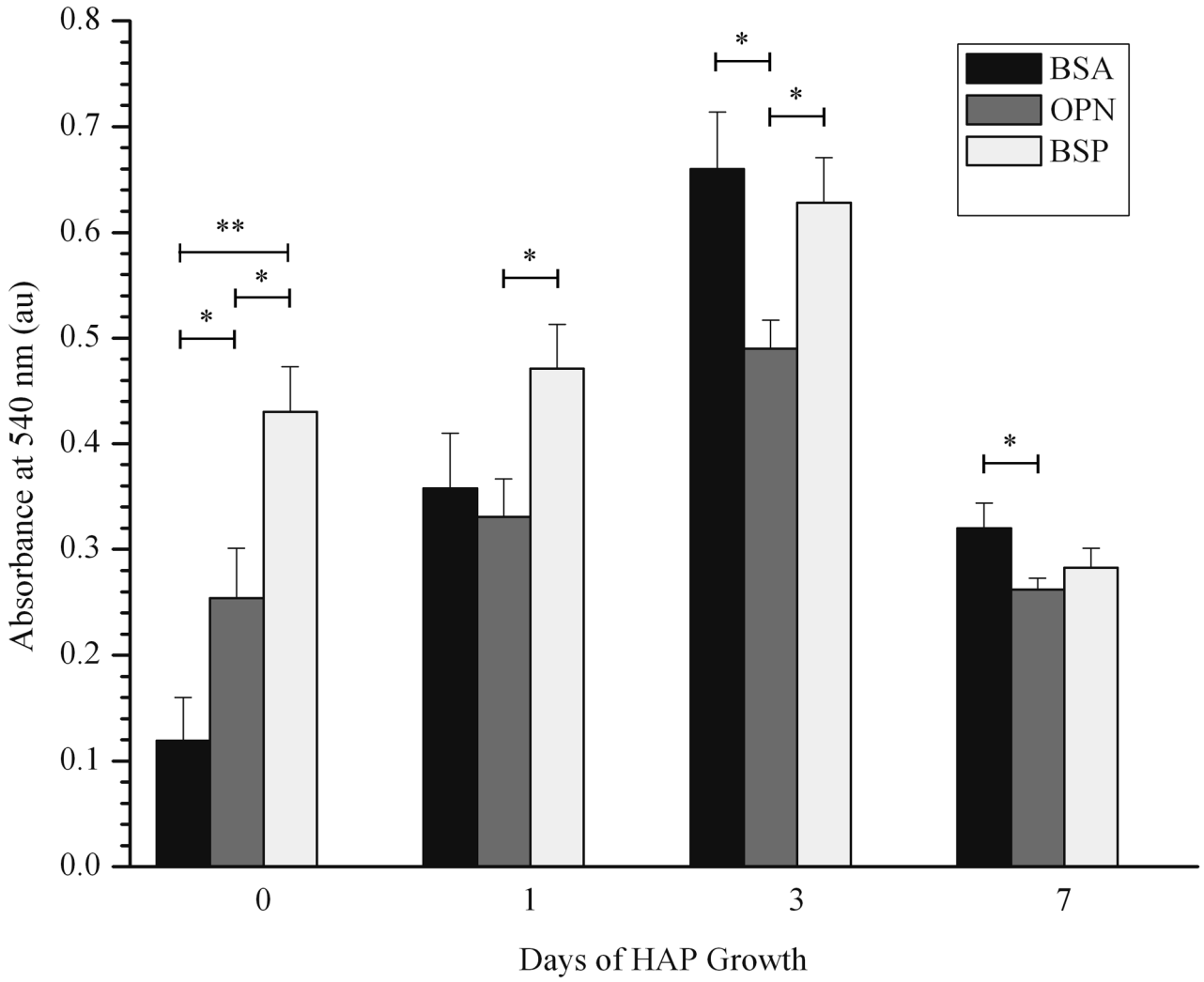

Figure 5.

Average MC3T3-E1 cellular adhesion to HAP substrates with adsorbed BSA, OPN, or BSP following a BSA blocking step, as measured with an MTT cell binding assay. The absorbance data are presented as the mean ± SE from at least nine samples completed over three separate occasions. * represents a statistically significant difference between the surfaces being compared with a confidence level of >95% ($p<0.05$). ** represents a statistically significant difference between the surfaces being compared with a confidence level of >99% ($p<0.01$).

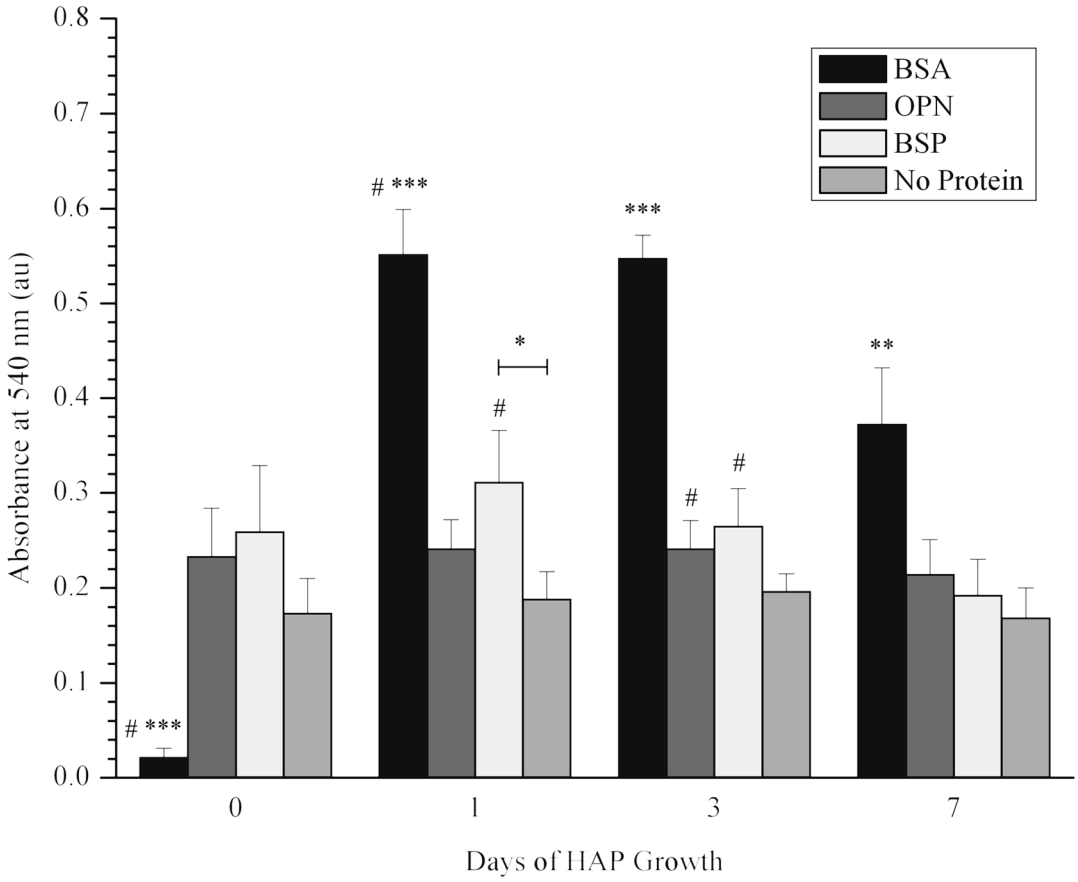

Figure 6.

Average MC3T3-E1 cellular adhesion to HAP substrates with adsorbed BSA, OPN, or BSP without a BSA blocking step, as measured with an MTT cell binding assay. The absorbance data are presented as the mean ± SE from at least twelve samples completed over four separate occasions. * represents a statistically significant difference between the surfaces being compared with a confidence level of >95% ($p<0.05$). ** represents a statistically significant difference between the indicated BSA case and all three of the other cases for that substrate with a confidence level of >95% ($p<0.05$). *** represents a statistically significant difference between the indicated BSA case and all three of the other cases for that substrate with a confidence level of >99% ($p<0.01$). # represents a statistically significant difference between the case indicated and the corresponding case from Figure 5 (BSA soaked) with a confidence level of >95% ($p<0.05$).

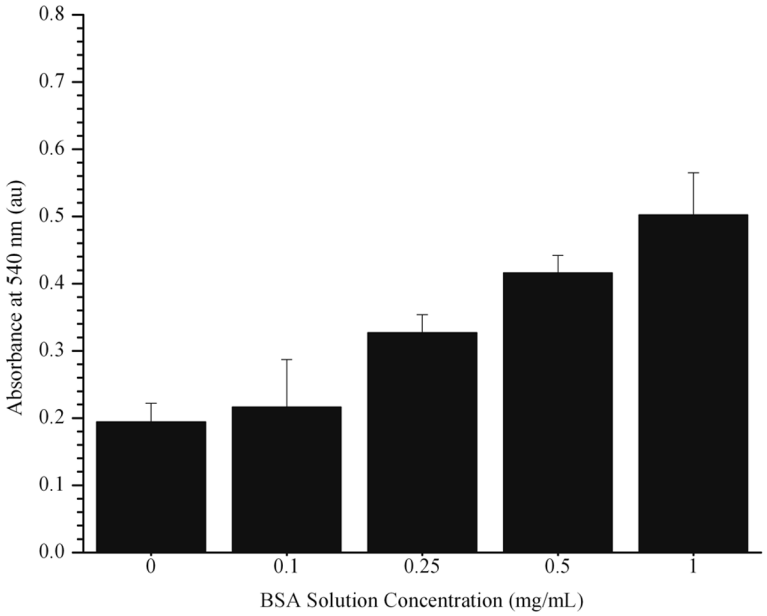

Figure 7.

MC3T3-E1 cellular adhesion to HAP grown for 3 days, following the adsorption of BSA from varying solution concentrations, as measured with an MTT cell binding assay. The absorbance data are presented as the mean ± SE from three samples.

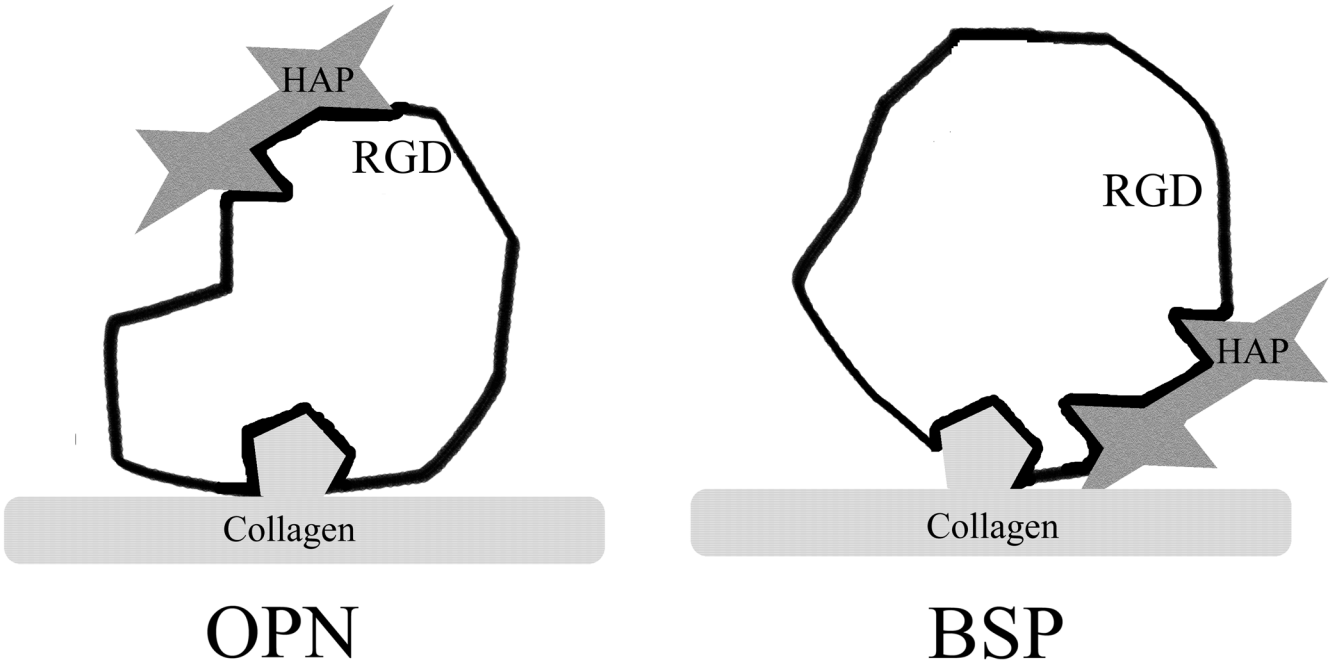

Figure 8.
The hypothesized locations of the collagen I and HAP binding regions relative to the RGD sequence in both OPN and BSP.

Table 1

Preparation Conditions for 500 mL of SBF [37]

Reagent	Quantity (g)
NaCl	2.7015
$NaHCO_3$	0.252
Na_2CO_3	0.213
KCl	0.1125
K_2HPO_4	0.115
$MgCl_2 \cdot 6H_2O$	0.1555
HEPES[a]	8.946[b]
$CaCl_2$	0.1465
Na_2SO_4	0.036
1.0 M NaOH	c

[a] 2-(4-(2-hydroxyethyl)-1-piperazinyl)ethanesulfonic acid.

[b] HEPES was dissolved in 50 mL of 0.2 M NaOH before addition.

[c] Added until pH = 7.4.

Table 2

Ca/P and O/Ca Ratios for HAP and Bone

Crystal Phase	Ca/P Ratios			O/Ca Ratios		
	Theory	**ESCA**	**EDAX**	**Theory**	**ESCA**	**EDAX**
Commercial HAP [45]	1.67	1.48	--	2.60	2.76	--
Bone [45]	--	1.49	--	--	3.20	--
1 Day HAP	--	--	1.24 ± 0.02	--	--	5.89 ± 0.49
3 Day HAP	--	--	1.39 ± 0.02	--	--	4.38 ± 0.14
7 Day HAP	--	--	1.52 ± 0.02	--	--	3.70 ± 0.11

Colloids Surf B Biointerfaces. Author manuscript; available in PMC 2009 July 15.